

The Force Acting on a Polymer Partially Confined in a Tube[†]

Peter Prinsen, Li Tai Fang, Aron M. Yoffe, Charles M. Knobler, and William M. Gelbart*

Department of Chemistry and Biochemistry, University of California, Los Angeles,
607 Charles E. Young Drive East, Los Angeles, California 90095-1569

Received: September 10, 2008; Revised Manuscript Received: December 17, 2008

We consider the force acting on a polymer part of whose length is configurationally confined in a tube and the rest of which is free. This situation arises in many different physical contexts, including a flexible synthetic polymer partially confined in a nanopore and a stiff viral genome partially ejected from its capsid. In both cases the force acting to pull the chain molecule out of its confinement is argued to be constant once a few persistence lengths are “free”/“outside”. We present Brownian dynamics simulations that confirm the constancy of the force for different chain lengths and illustrate the dependence of the force on the strength of tube confinement. Experimental results are reported for genome ejection from viral capsids, from which we estimate the pulling force to be a few tenths of a piconewton.

Introduction

Over the course of the past several years, attention has been focused on various mechanisms that facilitate the delivery of phage genomes to their bacterial hosts.¹ The process is often initiated by high pressure inside the capsid in which the viral DNA has been stored—high pressure predicted to arise from the self-repulsion and bending energy of the strongly confined DNA.² In several bulk-solution *in vitro* experiments, ejection of DNA from purified phage has been triggered by addition of the receptor molecule—a membrane protein from the bacterial host that opens the capsid upon binding to it. By setting up controlled osmotic “counter” pressures, the pressure in the capsid has been measured and found to be on the order of 50 atm, the precise value varying from one phage to another and dependent on ambient salt conditions.³ In the case of phage λ , for which several infectious mutants are known with different genome lengths but the same capsid size, the pressure has further been shown to increase with genome length.⁴ These results are consistent with single-molecule measurements of the force exerted by the motor protein that is responsible for packaging the phage genome into the preformed capsid.⁵ This force is found to increase to values on the order of 50 pN as the last end of the DNA is stuffed into the capsid. Indeed, integrating this force over the length of the genome gives a value of the stored energy density in agreement with the directly measured pressure in the fully packaged capsid. As with the bulk-solution measurements, this force has been shown to depend on salt concentration and genome length.⁶ The packaging forces and pressures are all related to the work that must be done to bend and compress the stiff, self-repelling DNA to close-packed densities.

In vivo, after binding to its receptor in the outer membrane of its host bacterium, the phage ejects its DNA into the cell. Because the osmotic pressure in the cytoplasm of the bacterial cell is several atmospheres,⁷ genome delivery is incomplete, for the same reasons it is incomplete in the above-mentioned *in vitro* experiments carried out in solutions with osmotic pressures of several atmospheres. More explicitly, for an osmotic pressure

of 3–4 atm, say, only about half of the λ genome is ejected; at this point, sufficient stress has been relieved in the capsid for the pressure inside to equal that outside, and there is no longer any net driving force for ejection. Accordingly, much effort has been devoted to elucidating different physical mechanisms that might complete the genome delivery process. One leading candidate, nicely established in the case of T7 phage, involves the transcription of early genes;⁸ RNA polymerase moves over the phage DNA in the usual way, but when it gets to the cell membrane where the phage capsid is bound, it begins to pull the DNA into the cell. In the case of T5,⁹ on the other hand, an early gene product of the virus essentially digests the host cell chromosome, thereby freeing an excess (with respect to the much smaller phage genome, only part of which is inside the cell at this point) of DNA-binding proteins; these then bind to the phage DNA and pull the part remaining in the capsid into the cell by thermal ratcheting.¹⁰

Another mechanism for pulling DNA out of phage capsids has been treated most recently,¹¹ involving osmotically induced condensation of the ejected DNA. More explicitly, ejection fractions have been measured in *in vitro* studies of purified phage λ in solutions containing osmolyte (high-molecular-weight poly(ethylene glycol), PEG) in the presence and absence of DNase, an enzyme that digests the ejected DNA into nucleotides but cannot reach the DNA remaining in the capsid. First, at each of several different PEG concentrations (osmotic pressures), the phages are opened by receptor molecules and allowed to “incubate” in the presence of DNase; the sample is then centrifuged, and the amount of DNA remaining in the supernatant—arising from the digested, ejected, DNA—is measured by UV absorbance. In this way, as in earlier experiments,³ the ejection fraction is determined to be a decreasing function of osmotic pressure, up to the point where the osmotic pressure is sufficient to completely suppress the ejection because it equals the pressure in the fully packaged capsid. These measurements were then repeated in the *absence* of DNase; the enzyme was added 1 h later, the solution spun down as before, and the amount of DNA in the supernatant measured. The ejection fractions at each osmotic pressure were consistently found to be higher than in the case where DNase was present from the outset. From this it is concluded that there is less DNA in the

[†] Part of the “PGG (Pierre-Gilles de Gennes) Memorial Issue”.

* To whom correspondence should be addressed: e-mail gelbart@chem.ucla.edu.

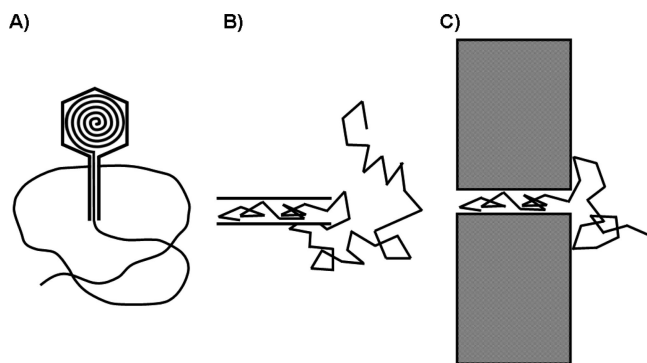


Figure 1. Schematic drawings of partially confined stiff (a) and flexible (b) chains in tubes and of a flexible chain in a tube through a planar wall (c).

capsid when the ejected length is allowed to remain intact. This difference is attributed to PEG-induced compaction of the ejected DNA giving rise to a net pulling force over and above the ejection and osmotic forces operative when the ejected chain is digested into nucleotides. *In vivo*, the situation is of course much more complicated because osmolarity and polyvalent cation concentrations vary widely.¹²

Each of the above scenarios is almost certainly operative to varying degrees in different instances of phage genome delivery into bacteria. In the present work we propose still another physical mechanism that we believe is also a likely driving force for pulling genomes into host cells after the capsid and osmotic pressures/forces are balanced. In particular, it is independent of the transcription and thermal ratcheting processes and is expected to be operative *in vivo* in cases where the osmotic conditions in the cell are not sufficient for DNA condensation to occur. It applies specifically in cases when the ejected chain is able to realize a significant amount of configurational disorder compared with its state in the capsid.

We calculate a “pulling” force that acts in any instance where one end of a chain molecule is geometrically constrained. This situation is depicted schematically in Figure 1a, for the case of genome ejection from a viral capsid. The tube shown here represents the hollow cylindrical “tail” of the virus, whose inner diameter is just large enough to accommodate a double-stranded DNA molecule; most of the genome is strongly confined—essentially hexagonally close-packed—in the “head” (capsid) of the phage particle. The DNA that has been ejected is able to enjoy configurational disorder, in contrast with its confined state in the virus. [Note that the persistence length of the DNA is larger than the inner radius of the capsid.] The lowering of the configurational free energy per unit length of ejected chain constitutes the entropic pulling force with which we are concerned in the present paper.

The scenario depicted schematically in Figure 1b is a closely related one but features a flexible chain that is partially confined in a cylindrical tube whose diameter is small compared with the polymer radius of gyration. A theoretical treatment of this system has just been reported by Klushin et al.,¹³ who present scaling analyses and Monte Carlo simulations for a flexible polymer pulled slowly by one end into a tube and subsequently released. We compare their results with those we obtain here in Brownian dynamics simulations of a flexible chain confined in a tube whose diameter is only slightly larger than the bead size of the polymer. Systematic experimental studies of this system have been performed by Craighead and co-workers,¹⁴ who use an electric field to drive a DNA molecule into a nanopore and then measure the properties of the “entropic recoil force” observed to pull it out upon turning off the field.

Finally, Figure 1c shows still another closely related physical situation in which the confining tube is embedded in a planar wall, so that the “free” portion of the chain is configurationally constrained by the wall. This scenario arises, for example, in the case of single-protein channels in lipid bilayer membranes, through which flexible linear polymers can be drawn in and out under conditions of strong chain-pore attraction. Recent experiments by Krasilnikov et al.¹⁵ investigate precisely this situation for α -hemolysin pores that transiently attract and confine high-molecular-weight PEG. They observe that residence times for the PEG molecules have a nonmonotonic dependence on polymer molecular weight, suggesting that a pulling force sets in as soon as the chain is long enough to fill the pore with some portion sticking outside. Indeed, this pulling force is similar to the one arising in Figure 1a,b but—as we argue in the Discussion—is not independent of the length of free chain because of the constraint arising from the wall.

We treat case 1a experimentally, deducing a value of the pulling force from comparison of ejection fraction measurements of a λ -phage genome in the presence and absence of DNase, as a function of osmotic pressure. The magnitude of the force is estimated to be a few tenths of a piconewton. Case 1b is treated via a Brownian dynamics simulation of flexible chains of different lengths that are partially confined in cylindrical tubes of different diameters only slightly larger than the polymer bead size. We show that the tension on the confined portion of chain—the “pulling force” acting on it due to the free portion—is independent of the overall chain length and of the length of free portion, depending only on the tube diameter.

Experimental Observation of Pulling Force

Here we present the experimental results from which we deduce the presence of a pulling force and make a preliminary estimate of its magnitude. Our experiments are similar to those recently reported by Jeembaeva et al.,¹¹ but for some important technical differences that we discuss in the final section.

In earlier work on phage λ we reported¹⁶ on the length of DNA remaining in the viral capsid as a function of osmotic pressure. Ejection of DNA was triggered by addition of the λ receptor molecule in the presence of osmolyte and DNase. The unejected DNA molecules were then released from the capsids by denaturation of the capsid protein in a phenol/chloroform mixture (which also “kills” the DNase), and their lengths were analyzed by pulsed-field gel electrophoresis. For each PEG concentration the unejected length was determined by a balance of forces involving the ejection force, f_{ej} —the force driving out the DNA along its length, due to the genome being crowded and bent on itself in the capsid—and the force f_{osm} pulling back on it because of the water inside being under tension due the presence of osmolyte outside. The osmotic force is constant during the ejection, fixed by the PEG concentration, while the ejection force decreases monotonically until the length remaining inside, L_{in} , allows $f_{ej}(L_{in}) = f_{osm}$.

We have repeated the above experiment but without DNase, i.e., allowing the ejected DNA to remain intact. After an hour, DNase is added and the lengths of DNA remaining in the capsids at that time are analyzed as outlined above. The results are shown in Figure 2 for four different PEG concentrations: 5% w/w (lanes 2 and 3), 10% (4 and 5), 15% (6 and 7), and 20% (8 and 9); lane 1 is a DNA calibration ladder, with lengths indicated in kilobase pairs (kbp). For each PEG concentration, the left (right) lane in the pair corresponds to the length measured in the presence [+] (absence [−]) of DNase. In each case there is a strong band at the top of the lane arising from

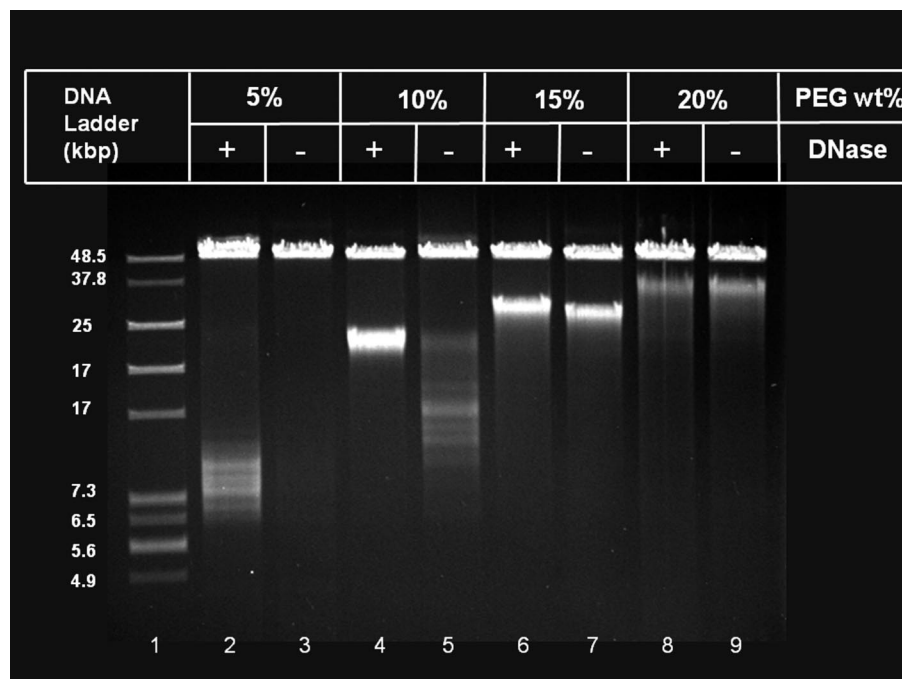


Figure 2. Pulsed-field gel electrophoresis showing the effect of the presence of DNase on the length of the genome remaining in the capsid at each of four different PEG concentrations. DNase was present during ejection in the lanes indicated by +; it was absent in the lanes indicated by -. The left-hand lane is a DNA calibration ladder. Twofold larger sample sizes were loaded into wells 2 and 3, in order to better image the differences between the with [+] and without [-] DNase situations.

the full-length (48.5 kbp) genome recovered from the capsids that were not opened by receptor molecules.

In lane 4 we see a band corresponding to a length of 20 kbp remaining in the capsid following ejection at 10% PEG in the presence of DNase, consistent with earlier measurements. In the absence of DNase, however, this sharp band is replaced by a diffuse band corresponding to a spread of lengths around 12 kbp (see lane 5); i.e., the intact ejected DNA has pulled out an additional 6–10 kbp of DNA from the capsid. More explicitly, the force balance $f_{ej}(L'_{in}) = f_{os}$ (≈ 0.6 pN for 10% PEG¹⁷) achieved for a length $L_{in} = 20$ kbp is replaced by the balance $f_{ej}(L'_{in}) = f_{osm} - f_{pull}$ with $L'_{in} \approx 12$ kbp. Note that f_{pull} and f_{osm} both remain constant throughout the ejection process, the latter fixed by the constant PEG concentration and the former by the fact that—as we argue in the next section—the pulling force is independent of free (ejected) chain length as soon as a few persistence lengths are free. From these results at 10% PEG we learn that f_{pull} is lower than 0.6 pN ($= f_{osm}$, at this PEG concentration) because otherwise *no* DNA would have been found in the capsid in the absence of DNase at this PEG concentration.

We can similarly obtain a *lower* bound on f_{pull} by analyzing the results obtained for 5% PEG. The diffuse band in lane 2 corresponds to an unejected length of 7–9 kbp, consistent with earlier measurements. The absence of any band in lane 3 (other than that at the top, from unopened capsids), however, indicates that these 7–9 kbp of DNA are completely pulled out from the capsid when DNase is not present, i.e., when the ejected DNA remains intact. Because f_{osm} is about 0.2 pN at this concentration of PEG (5%) and because the pulling force is sufficient to overcome this osmotic force, we can infer that f_{pull} is at least as large as $f_{osm} \approx 0.2$ pN.

Armed with the conclusion that f_{pull} must be a few tenths of a piconewton, we can understand immediately the results obtained at the higher PEG concentrations. Lanes 6 and 7, for example, show that about 27 kbp of DNA remain in the capsid

at 15% PEG in the absence of DNase and that only a little less (25 kbp) remain in its presence. This is consistent with f_{pull} being small compared with f_{osm} (≈ 1.3 pN) at this osmolyte concentration, so that $f_{ej}(L'_{in}) = f_{osm} - f_{pull}$ reduces essentially to $f_{ej}(L_{in}) = f_{osm}$. At 20% PEG, where f_{osm} (≈ 2.1 pN) is still larger, the extra pulling force is completely overwhelmed by f_{osm} , consistent with lanes 8 and 9 both showing 35 kbp remaining in the capsid.

Theory of Pulling Force

Heuristic Arguments. Consider a limiting case of Figure 1b in which the confined portion of an ideal flexible chain is *completely* constrained. Then all of the configurational disorder of the chain arises from the free portion (of length L_{out}) whose entropy can be written as $S = k_B \ln \Omega$, $\Omega = c^{N_{out}}$, with k_B the Boltzmann constant, c an effective coordination number, and $N_{out} = L_{out}/\xi$ the number of uncorrelated links of length ξ . It follows that the configurational free energy of the overall chain, relative to its value when completely constrained, is $F = -TS = -k_B T(L_{out}/\xi) \ln c \approx (-k_B T/\xi)L_{out}$ and that the effective, entropic, force converting constrained to free chain is $f_{pull} = -\partial F/\partial L_{out} \approx k_B T/\xi$, independent of L_{out} .

When the confined portion of the chain is *not* completely constrained, an estimate of the pulling force can be obtained quite generally from solution of the corresponding diffusion equation. In the case of an ideal chain partially confined in a tube of diameter $d > \xi$, for example, one finds the result¹⁸ $F \approx \text{const} - \gamma k_B T(R_g/d)^2$, where $R_g^2 \approx L_{out}\xi$ is the square of the radius of gyration of the free portion of the chain and γ is a numerical factor of order unity. Here F is again the free energy of the overall chain, relative to its value when constrained, and hence $f_{pull} = -\partial F/\partial L_{out} \approx (k_B T/\xi)(\xi/d)^2$. The force is again independent of the ejected length L_{out} , as in the above estimate, but is smaller than before by a factor of $(\xi/d)^2$ (note that $d > \xi \Rightarrow f_{pull} < k_B T/\xi$) because configurational disorder has not been completely suppressed in the confined portion of chain. For stiff

chains, with persistence length ξ exceeding the width d of the confining tube, the confinement free energy and associated pulling force depend again on both ξ and d , but now through the Odijk deflection length,¹⁹ $\lambda \equiv \xi^{1/3}d^{2/3}$. But the pulling force will still be independent of the length of free chain, once several persistence lengths are free, and only its magnitude will be affected.

Phenomenological Simulations. To illustrate the basic physics of the pulling force described above under conditions of strong confinement, we have performed Brownian dynamics (BD) simulations²⁰ on an ideal flexible chain confined in an open cylindrical pore whose diameter is only slightly larger than the monomer size. The case of a more weakly confined flexible chain has been treated by Klushin et al.¹³ (see Discussion).

The flexible chain is modeled as a string of N overlapping beads, each connected by harmonic springs to its nearest neighbors. The equilibrium interbead bond length l is taken as the unit of length. The unit of energy is $k_B T$, and the unit of time is $l^2\mu/k_B T \equiv \tau$, where μ is the friction coefficient of a single bead. The diameter of each bead is 2 in dimensionless units, and the beads interact with each other only through their connecting springs; i.e., no excluded volume interactions are involved. They do, however, interact with the half-infinite cylindrical pore whose axis coincides with the x -direction and which is open at its right end ($x = 0$). The thickness of the cylindrical wall is zero, but it has a hard interaction with beads both inside and outside the cylinder; i.e., the center of a bead cannot come closer than unit distance to the cylinder wall.

BD simulations are performed in the usual way.²⁰ At each time t we calculate the total force on each bead (due to the springs connecting it to its nearest neighbors). The force \vec{f}_i on the i th bead due to the $(i - 1)$ th bead, for example, is $-k[(\vec{x}_i - \vec{x}_{i-1}) - 1](\vec{x}_i - \vec{x}_{i-1})/|\vec{x}_i - \vec{x}_{i-1}|]$, where \vec{x}_i is the position of bead i and k is the spring constant. A new position (for time $t + \delta t$) is then assigned to bead i according to

$$\vec{x}_i(t + \delta t) = \vec{x}_i(t) + \vec{f}_i(t)\delta t + \delta\vec{X}_i \quad (1)$$

Here $\delta\vec{X}_i$ is a Gaussian random displacement associated with the time step δt , with zero mean and with variance given by $\langle\delta X_{i\alpha}\delta X_{j\beta}\rangle = \delta_{ij}\delta_{\alpha\beta}2\delta t$, $i, j = 1, 2, \dots, N$ and $\alpha, \beta = x, y, z$. Note that we have taken $\mu = 1$ and $k_B T = 1$ in dimensionless units, so that the diffusion coefficient $D = k_B T/\mu$ for a bead is also 1. The choice of δt is limited by the value of the spring constant k . If it is too large, the average energy per spring will exceed its equipartition value of $1/2$ and the simulation can become unstable; if it is too small, the simulation is inefficient. We use $k = 50$ and $\delta t = 10^{-4}$ (for which we find an average energy per spring within 0.2% of $1/2$).

To keep the beads from overlapping with the cylinder wall, i.e., from coming closer to it than a unit distance, we use a device developed by Tao et al.²¹ Suppose that at some time t a time-step displacement performed according to eq 1 would result in overlap of the bead with the wall. Instead of making the move, we determine $0 < \lambda < 1$ such that the bead would just touch the wall at time $\lambda\delta t$; i.e., we choose the $\delta\vec{X}_i$ from the same Gaussian distribution as before but replace δt by $\lambda\delta t$ in eq 1 and perform the corresponding displacement. If bead i is inside the cylinder at time t , then λ is a solution of

$$[y_i(t + \lambda\delta t)]^2 + [z_i(t + \lambda\delta t)]^2 = \left[\frac{d}{2} - 1\right]^2 \quad (2a)$$

with

$$y_i(t + \lambda\delta t) = y_i(t) + f_{iy}(t)\lambda\delta t + \sqrt{\lambda}\delta X_{iy} \quad (2b)$$

and an identical equation for $z_i(t + \lambda\delta t)$. Similar relations are used for the other two cases of bead-wall interaction that arise, namely a bead approaching from outside or from near the entrance of the tube, relevant to times after which part of the chain has exited the tube. There are four solutions to eqs 2a and 2b, but we use only the smallest positive real solution for λ , generate a new random displacement $\delta\vec{X}_i$, and complete the time step according to

$$\vec{x}_i(t + \delta t) = \vec{x}_i(t + \lambda\delta t) + \vec{f}_i(t)(1 - \lambda)\delta t + \sqrt{1 - \lambda}\delta\vec{X}_i \quad (1a)$$

If this again leads to overlap with the wall, we repeat the procedure until a complete time step has been performed.

To calculate the pulling force associated with partially confined chains, we fix one end-bead at a certain x -position ($x_1 < 0$) inside the tube whose right, open, end is at the origin. For a given value of N (the number of beads) and of d , we start the computation by choosing an initial configuration for the chain: $\vec{x}_i = (x_1 + (i - 1), 0, 0)$, $1 \leq i \leq N$. We simulate until the center-of-mass position of the chain fluctuates around a constant value, typically on the order of 10^8 time steps, and then simulate for another 10^8 time steps (for $N = 100$) or 3×10^8 time steps (for $N = 200$ and 300), during which we measure the x -component of the force on the fixed bead. We also measure the corresponding average number of beads outside the tube.

Figure 3 shows the average x -component of the above force vs. the average number of beads outside for different chain lengths ($N = 100$ [\times], 200 [\circ], 300 [$+$]) and tube diameters ($d = 3, 4, 5$). Note that the force is essentially independent of chain length, whereas it is a decreasing function of tube diameter. Once some length protrudes from the tube, the pulling force is constant, depending only on the strength of tube confinement.

Discussion

We have shown that the free portion of a partially confined flexible chain in a tube exerts a constant force pulling on the rest of the chain and have determined from BD simulations how this force decreases with increasing tube diameter.

Recently published analyses by Klushin et al.¹³ treat the case of a flexible chain that is “weakly” confined in the sense that the tube diameter is large compared to the monomer size. In this limit the confined portion of the chain can be described by a string of nonoverlapping “blobs”²² of size d , each consisting of a large number of monomers, and Monte Carlo simulation results are shown to agree well with scaling relations. Free energies (relative to those of free, unconfined, coils) are calculated for a partially confined chain one of whose ends has been fixed at a distance x inside the tube. For each chain length and tube diameter, this free energy increases linearly with x until a critical x value (which is *greater* than the average end-to-end distance of the *fully* confined chain, i.e., one with no tension on it due to an outside, free, portion); at this point the free energy equals that of the fully confined chain. When the chain has been “dragged” into the tube this far, the rest of the chain will spontaneously be “slurped” in via a discontinuous first-order phase transition. In the opposite direction—starting

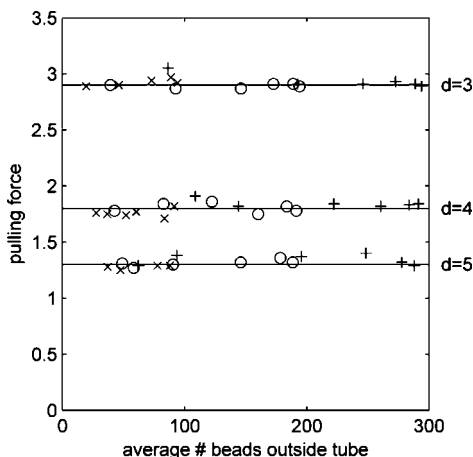


Figure 3. BD simulation results for pulling force vs. average number of beads outside the confining tube, for different chain lengths ($N = 100$ [\times], 200 [\circ], 300 [$+$]) and different tube diameters ($d = 3, 4, 5$). The horizontal lines correspond to pulling forces of 1.3, 1.8, and 2.9. The average force is the same for all chain lengths but increases with strength of confinement; estimated errors are about 0.05.

with x large enough that the chain is fully confined in the tube—the release of the chain is shown to be continuous.

Our attention to pulling forces acting on partially confined chains was drawn by experiments investigating the different degrees of osmotic suppression of phage ejection in the presence and absence of an enzyme that digests the “free” portion of the DNA genome. We have chosen to analyze this effect by neglecting the role of osmolyte in condensing the ejected chain; i.e., we have treated the case of a chain that is configurationally free upon exiting its confining geometry (see the scenarios depicted in Figure 1a,b).

Upon completing our work, we learned of a series of experimental studies by Craighead and co-workers¹⁴ that address directly the pulling force arising from partial confinement of a semiflexible polymer. They create a microfluidic device, half of which is “pillared”; i.e., pillars about 35 nm in diameter, separated from one another by about 100 nm, fill half of an ~ 100 nm high slab. The remaining half of the slab is free of these constraints. Semiflexible polymers—50 μm long DNA molecules, fluorescently labeled—are introduced into the free region, and an electric field is applied perpendicular to the interface between the pillared and free regions, in the plane of the microfluidic slab. The field draws the molecules into effective 100 nm diameter nanotubes between the pillars, parallel to the field direction. Upon turning off the field the partially confined molecules are observed to be pulled out of the pillared region, and the force driving this “recoil” is ascribed to the configurational entropy of the free portion of the chain. From the measured velocities and an estimate of the drag coefficient of the DNA chain in this environment, they are able to deduce a lower bound on the entropic pulling force of about a hundredth of a piconewton, close to what one would estimate from the entropy difference (k_B per Kuhn length) between the pillared and free regions. They also conclude (as we found above) that the force is independent of the length of the molecule. Interestingly, in addition, it is pointed out that shorter molecules will be pulled *completely* into the pillared region during the time that the electric field is on, implying that they will remain there longer than partially confined, longer, molecules (since there is no force pulling on them), thereby providing a basis for chain separation.

As mentioned in the Introduction, a similar physical situation is realized in measurements performed by Krasilnikov et al.¹⁵

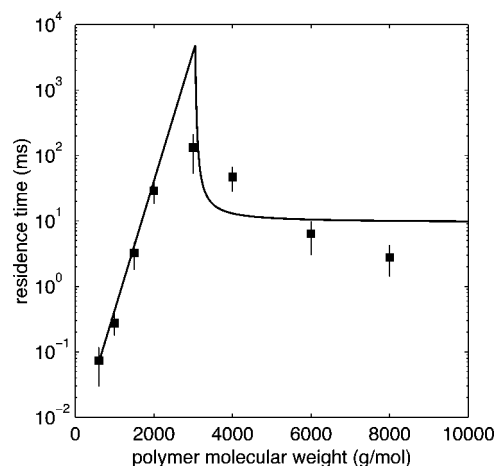


Figure 4. Average residence time for a flexible chain in a cylindrical pore as a function of polymer molecular weight. The dots show the data from the Krasilnikov et al.¹⁵ measurements, while the curve indicates the behavior predicted by the simplest theory of a flexible chain partially confined in an attractive pore with the geometry shown in Figure 1c (see Discussion in text, surrounding eq 3b).

on the motion of a flexible polymer in and out of a confining pore in a planar membrane. Experiments were carried out for each of several different molecular weights of polymer, and the average residence time was found to increase at first with molecular weight and then go through a maximum, as shown by the data points in Figure 4. By applying the ideas outlined above, we can account simply for this behavior and predict further that the residence time should decrease to an asymptotic value at still higher values of molecular weight (see the curve in Figure 4).

From current vs time traces associated with the transient blocking of single pores by PEG molecules, Krasilnikov et al. determine the average residence time τ under conditions where the molecule–pore attraction is strong and the escape kinetics are determined by an effective energy barrier according to

$$\tau \propto e^{\Delta F(N)} \quad (3)$$

$$\Delta F(N) = \chi N \quad (3a)$$

Here $\Delta F(N)$ is the magnitude of the free energy (in units of $k_B T$) of a chain of N monomers, relative to its value outside, and $\chi > 0$ is the energy lowering per monomer due to the attraction between the chain and the pore. As Krasilnikov et al. point out, this accounts for the initial linear rise in the semilog plot of average residence time vs. N (molecular weight). In remarking on the presence of a maximum, they correctly invoke an entropic pulling force arising from the fact that higher molecular weights necessarily involve a portion of the polymer outside the pore. They estimate this force to be on the order of a few piconewtons by likening it to the entropic force required to pull apart the two ends of a flexible polymer. A more appropriate description, however, is obtained by treating the “free” portion of the chain as a polymer attached at one end to a planar wall (see Figure 1c). Note that while, technically, the free portion is not actually attached to the wall, it is effectively constrained in this way because it is attached to the portion that is strongly confined in the tube and whose end is essentially fixed at the wall.

We estimate the pulling force associated with scenario 1c by a simple generalization of the argument made earlier for the

no-wall case (1b) of the freeing of a flexible polymer from a confining tube. Instead of describing the free-chain partition function—the number of available configurations—by the estimate $c^{N_{\text{out}}}$, we simply include the multiplicative factor correcting²³ for the presence of a wall; i.e., we use $\Omega = N_{\text{out}}^{-1/2} c^{N_{\text{out}}}$ for the number of configurations available to a flexible chain, one of whose ends is tethered to a planar wall. Recall that c is an effective coordination number with $\ln(c)$ a numerical factor of order unity and that $N_{\text{out}} = L_{\text{out}}/\xi$ is the number of persistence lengths outside the pore. It follows that the associated pulling force is no longer independent of N_{out} : $f_{\text{pull}} = -\partial F/\partial L_{\text{out}} \approx (kT/\xi)(1 - 1/2N_{\text{out}})$. Accordingly, we modify eq 3a to include the energy $f_{\text{pull}}\Lambda$ associated with the pulling force:

$$\Delta F(N) = \chi N, N \leq N^* \\ = \chi N^* - \frac{\Lambda}{\xi} \left(1 - \frac{1}{2(N - N^*)} \right), N > N^* \quad (3b)$$

Here Λ is the length of the pore and N^* is the number of monomers at which the chain completely fills the pore.

Substituting eq 3b into eq 3 gives the curve in Figure 4. To produce the plot, we take the ratio of pore length to chain persistence length to be 6, consistent with $\Lambda \approx 6$ nm and $\xi \approx 1$ nm. Since each monomer ($\text{CH}_2\text{CH}_2\text{O}$) has a length of about 0.4 nm and a molecular weight of 44 Da, one persistence length consists of 2.5 monomers and has a molecular weight of 110 Da. The number of segments N can then be calculated from $N = W/110$, where W is the molecular weight of the polymer in Da. For χ and W^* we use the experimental values¹⁵ of 0.2 (in units of $k_B T$) and 3000 g/mol determined respectively from the initial slope of $\log(\tau)$ vs. W and from the molecular weight at which the pore conductance saturates. The discontinuous drop from the maximum at $W^* = 3000$ is a consequence of our simplified model in which the confined portion of chain is denied any configurational entropy. In contrast, the experimental data (squares) go smoothly through the maximum because of the significant disorder possible for the chain even when it is in the pore. The residence times are predicted not only to go through a maximum but also to level off to a constant value at sufficiently high molecular weight. Note that the effective attraction energy (in units of kT), $\chi N^* - f_{\text{pull}}\Lambda$, is always positive and that f_{pull} is a maximum at the point where the polymer first begins to feel a pulling force, i.e., when it completely fills the pore to which it is strongly attracted.

Finally, we return to the osmotic suppression experiments involving phage ejection and the chain condensation effects associated with the presence of PEG in the solution. As mentioned earlier, Jeembaeva et al.¹¹ have recently carried out experiments of this kind, as part of a general study of the effects of osmotic pressure and DNA-binding proteins on the extent of genome delivery by phage.

In the absence of DNase they found a nonmonotonic dependence of ejection fraction on PEG concentration. More explicitly, for 48.5 kbp λ -DNA, they report ejection fractions of 100%, 60%, 70%, and 0% for PEG concentrations (w/w) of 5%, 15%, 20%, and 30%. In the presence of DNase they measured ejection fractions of 90%, 50%, 40%, and 0%, respectively, for these same PEG concentrations. We find, on the other hand, that the ejection fractions decrease monotonically with PEG concentration for experiments carried out both in the presence and in the absence of DNase, with the fractions simply being larger in the latter case. Specifically, in the absence of DNase, we find (see Figure 2) ejection fractions of 100%, 70%, 46%, and 28% at PEG concentrations of 5%, 10%, 15%, and

20%, whereas in the presence of DNase we find 80%, 55%, 44%, and 28%. That is, we find monotonic decreases in both cases and that as soon as the PEG concentration is as high as 15% or 20%, the osmotic pressure is large enough for the “extra” pulling force to be overwhelmed by f_{osm} . (At 30% PEG the ejection fractions are trivially the same (0%), with or without DNase, because there is no chain outside and therefore no pulling force.)

From cryo-electron microscopy Jeembaeva et al. have deduced that the ejected portions of DNA are condensed at all PEG concentrations involved. Accordingly, they argue that pulling forces observed in their experiments arise from PEG-induced DNA condensation. Outside the capsid, the free energy of condensation is moderated by the usual bending and surface contributions; inside, direct interactions with and confinement by the capsid are operative. They conclude in this way that the effective pulling force—the difference between the osmotic effects on the DNA–DNA interactions inside and outside—increases with PEG concentration, thereby accounting for their observation of a minimum (followed by a maximum) in the ejection fraction as a function of PEG. Their determinations of ejection fractions at different osmotic pressures involve measurements of UV absorbances by digested DNA remaining in the supernatant following centrifugation of the nuclease-treated sample. Ours, on the other hand, involve pulsed-field gel electrophoresis measurements of the length remaining in the opened capsids. The two sets of experiments are in agreement, except in the single case of ejection fraction measured at 20% PEG in the absence of DNase, where they report a value significantly (more than 2 times) larger than ours, large enough to give their reported nonmonotonic behavior. Apart from this one instance, their measured ejection fractions are no more than 20% larger than ours, consistent with the fact that UV absorbance measurements had been found earlier¹⁶ to be about this much larger than those determined by gel electrophoresis. When we perform ejection fraction determinations by measuring UV absorbances of the supernatants, we do not find the nonmonotonic behavior reported by Jeembaeva et al.—but, again, it is only because at 20% we find a significantly smaller value than theirs. Finally, it should be noted that each set of measurements performed by both groups has been repeated several times, with measured ejection fractions varying from one phage batch to another by 10–15%.

In summary, we have presented experimental and computational results determining the force acting on a linear polymer when a portion of it is configurationally constrained in a tube. This force is expected to be operative under a wide variety of confinement and chain flexibility conditions and to be independent of the fraction confined and of the overall chain length. The magnitude of the force is a few tenths of a piconewton and large enough to show observable physical effects, such as the completion of viral genome delivery discussed here. It is likely that still other mechanisms are yet to be identified as contributing to this fundamental biological process and that in many *in vivo* instances several of them will be simultaneously operative in a way that is difficult to unravel. Further elucidation of the basic physics underlying each of them should therefore be useful in clarifying the situation.

Acknowledgment. The work described in this paper was partially supported by the U.S. National Science Foundation (Grant CHE 0714411, to W.M.G. and C.M.K.). P.P. acknowledges support from a Rubicon grant from The Netherlands Organisation for Scientific Research, and A.M.Y. has benefited from a UCLA Dissertation Year Fellowship.

References and Notes

- (1) Gonzalez-Huici, V.; Salas, M.; Hermoso, J. M. *Mol. Microbiol.* **2004**, *52*, 529–40.
- (2) (a) Kindt, J.; Tzlil, S.; Ben-Shaul, A.; Gelbart, W. M. *Proc. Natl. Acad. Sci. U.S.A.* **2001**, *98*, 13671–4. (b) Tzlil, S.; Kindt, J. T.; Gelbart, W. M.; Ben-Shaul, A. *Biophys. J.* **2003**, *84*, 1616–27.
- (3) Evilevitch, A.; Lavelle, L.; Knobler, C. M.; Raspaud, E.; Gelbart, W. M. *Proc. Natl. Acad. Sci. U.S.A.* **2003**, *100*, 9292–5.
- (4) Grayson, P.; Evilevitch, A.; Inamdar, M. M.; Purohit, P. K.; Gelbart, W. M.; Knobler, C. M.; Phillips, R. *Virology* **2006**, *348*, 430–2.
- (5) Smith, D. E.; Tans, S. J.; Smith, S. B.; Grimes, S.; Anderson, D. L.; Bustamante, C. *Nature (London)* **2001**, *413*, 748–52.
- (6) Fuller, D. N.; Rickgauer, J. P.; Jardine, P. J.; Grimes, S.; Anderson, D. L.; Smith, D. E. *Proc. Natl. Acad. Sci. U.S.A.* **2007**, *104*, 11245.
- (7) Early work measuring osmotic pressure in bacterial cells suggests values of 3–4 atm see, for example: Stock, J. B.; Rauch, B.; Roseman, S. *J. Biol. Chem.* **1977**, *252*, 7850–61.
- (8) Garcia, L. R.; Molineux, I. J. *J. Bacteriol.* **1995**, *177*, 4066–76.
- (9) Berget, S. M.; Mozer, T. J.; Warner, H. R. *J. Virol.* **1976**, *18*, 71–9.
- (10) Cordova, N. J.; Ermentrout, B.; Oster, G. F. *Proc. Natl. Acad. Sci. U.S.A.* **1992**, *89*, 339–43.
- (11) Jeembaeva, M.; Castelnovo, M.; Larsson, F.; Evilevitch, A. *J. Mol. Biol.* **2008**, *381*, 310–23.
- (12) Odijk, T. *Biophys. Chem.* **1998**, *73*, 23–9.
- (13) Klushin, L. I.; Skvortsov, A. M.; Hsu, H.-P.; Binder, K. *Macromolecules* **2008**, *41*, 5890–5898.
- (14) Turner, S. W. P.; Cabodi, M.; Craighead, H. G. *Phys. Rev. Lett.* **2002**, *88*, 128103/1–4.
- (15) Krasilnikov, O. V.; Rodrigues, C. G.; Bezrukov, S. M. *Phys. Rev. Lett.* **2006**, *97*, 018301.
- (16) Evilevitch, A.; Gober, J. W.; Phillips, M.; Knobler, C. M.; Gelbart, W. M. *Biophys. J.* **2005**, *88*, 751–6.
- (17) Evilevitch, A.; Fang, L. T.; Yoffe, A. M.; Castelnovo, M.; Rau, D. C.; Parsegian, V. A.; Gelbart, W. M.; Knobler, C. M. *Biophys. J.* **2008**, *94*, 1110–20.
- (18) (a) Casassa, E. F. *J. Polymer Sci. B* **1967**, *5*, 773–8. (b) De Gennes, P. G. *Scaling Concepts in Polymer Physics*; Cornell University Press: Ithaca, NY, 1979.
- (19) Odijk, T. *Macromolecules* **1983**, *16*, 1340–1344; **1984**, *17*, 502–503.
- (20) Allen, M. P.; Tildesley, D. J. *Computer Simulations of Liquids*; Oxford University Press: New York, 1989.
- (21) Tao, Y.-G.; Den Otter, W. K.; Dhont, J. K. G.; Briels, W. J. *J. Chem. Phys.* **2006**, *124*, 134906.
- (22) (a) Daoud, M.; de Gennes, P. G. *J. Phys. (Paris)* **1977**, *38*, 85. (b) Brochard-Wyart, F.; Hervet, H.; Pincus, P. *Europhys. Lett.* **1994**, *26*, 511–6.
- (23) DiMarzio, E. A. *J. Chem. Phys.* **1965**, *42*, 2101–6.

JP808047U